Comparison of Pentacene and Amorphous Silicon AMOLED Display Driver Circuits

Vaibhav Vaidya, *Student Member, IEEE*, Susan Soggs, Jungbae Kim, Andreas Haldi, Joshua N. Haddock, Bernard Kippelen, and Denise M. Wilson, *Member, IEEE*

***Abstract*—Organic light-emitting diode (OLED) displays offer distinct advantages over liquid crystal displays for portable electronics applications, including light weight, high brightness, low power consumption, wide viewing angle, and low processing costs. They also are attractive candidates for highly flexible substrates. In active-matrix OLED (AMOLED) displays, a small transistor circuit is used to drive each OLED device. This paper compares the simulated performance of two state-of-the-art AMOLED drivers with a proposed 5 thin-film-transistor (TFT) voltage programmed driver circuit which combines the advantages of the first two configurations. A competitive evaluation is also done between amorphous silicon (α-Si) and organic TFTs (OTFTs,) using comparable empirical device models for α-Si) and pentacene OTFTs. The 5-TFT circuit is found to match the speed of the 2-TFT while achieving a stability closer to the 4-TFT circuits and demonstrating a better speed-stability tradeoff.**

***Index Terms*—Active-matrix (AM) display drivers, amorphous silicon (α-Si), analog integrated circuits, AM organic light-emitting diode (AMOLED), OLEDs, organic electronics, organic thin-film transistor (OTFT), TFTs, pentacene.**

I. Introduction

Organic **l**ight-**e**mitting **d**iode (OLED) displays offer advantages for portable electronics applications such as light weight, high brightness, low power consumption, wide viewing angle, and low processing costs over the **l**iquid **c**rystal **d**isplays (LCDs), which currently dominate the market [12]. These properties have focused attention on OLEDs for use in the next generation of flat-panel displays. Implementing flat-panel displays presents the technical challenge of driving a large number of pixels to form a coherent display addressed by a moderate number of external data lines. Further, implementing such displays with OLEDs adds further complexity due to the characteristics of OLED devices. As a result, innovative schemes are needed to drive the OLED pixels [19]. Displays based on OLEDs are addressed either passively or actively, in the tradition of passive-matrix and active-matrix (AM) displays based on liquid crystal and competing technologies. In a passive addressing scheme, the display is addressed one line at a time, which means that in a display with 300 lines, a pixel can only be energized for 1/300th of the total display time. The OLED must then be driven to a high instantaneous brightness, because no active interim drive current is applied and therefore the pixel voltage decays as the OLED capacitance discharges. Despite these drawbacks, the main advantages of passively addressed displays are low cost and simplicity [19].

An increasing percentage of displays are based on active matrix addressing, in which **t**hin-**f**ilm **t**ransistor (TFT) circuits are used to continuously drive each pixel. A relatively small steady current is used to drive an AM pixel, rather than an instantaneous pulse of higher current as in a passive addressing scheme. Each pixel remains on after the end of the program pulse because TFT circuits have analog memory and maintain drive current even when individual pixels are not addressed. OLED quantum efficiency is greater at the lower drive current densities used in the active driver configuration; thus, overall power consumption is decreased and OLED lifetime is increased. In addition, active addressing schemes eliminate the issue of crosstalk caused by reverse bias leakage currents seen in passive addressing [1].

In designing AM displays with OLEDs, organic transistor materials offer many of the same advantages as OLEDs including light weight, inherent mechanical flexibility, and compatibility with flexible substrates, as well as lower cost processing. Organic transistors are fabricated with the same tools and processes as OLEDs, so a combined fabrication process may be more easily implemented and, thus, may offer additional manufacturing advantages. However, the bulk of the current AMOLED display driver literature is focused on **a**morphous **Si**licon (α-Si) TFTs, likely because **o**rganic TFTs (OTFTs) have long been perceived as having two main disadvantages compared to α-Si TFTs: 1) low device mobilities and 2) material instability/degradation over time. In addition, α-Si is perceived as being able to take advantage of a mature processing industry. However, a re-examination of current literature comparing OTFT and α-Si TFT devices and processes shows that these perceptions may now be considered dated, especially for highly flexible AM display applications.

The gap between OTFT and α-Si TFT process technologies is closing for two reasons: 1) limited mobility in low temperature α-Si fabricated on flexible substrates and 2) material and fabrication advances in organic materials. Very low temperature processes ($<150^{\circ}$C) are necessary for the fabrication of circuits on plastic substrates for highly flexible or optically clear target applications. The results for low temperature α-Si in terms of

Manuscript received December 14, 2006; revised July 24, 2007. This work was supported in part by the STC program of the National Science Foundation under Agreement DMR 0120967, by the Office of Naval Research, in part by the Microelectronics Research Center,Georgia Institute of Technology, a member of the National Nanotechnology Infrastructure Network, supported by the NSF under Grant ECS- 03-35765. This paper was recommended by Associate Editor M. E. Zaghloul.

V. Vaidya, S. Soggs, and D. M. Wilson are with the Department of Electrical Engineering,University of Washington, Seattle, WA 98195-2500 USA (e-mail: denisew@u.washington.edu).

J. Kim, A. Haldi, J. N. Haddock, and B. Kippelen are with the School of Electrical and Computer Engineering, Georgia Institute of Technology, Atlanta, GA 30332-0250 USA.

Digital Object Identifier 10.1109/TCSI.2008.916548

mobility as well as degradation have been inconsistent, with reported mobilities of 0.5 to 0.8 cm^2/V-s [1], [2]. On the other hand, the field-effect mobility of pentacene-based transistors has recently been routinely demonstrated to be on the order of 1.0 cm^2/V-s [3], which approaches the mobility of high temperature α-Si devices. At the same time, the encapsulation of organic thin films to prevent the film degradation effects of atmospheric exposure has been an active area of research, and inorganic or stacks of organic/inorganic thin-film passivation layers have been shown to greatly increase the stability of organic semiconductor thin films [4]–[6]. Progress has also been made in the development of organic passivation materials that exhibit decreased permeability to atmospheric gases and water; such permeability has shown to be the source of organic semiconductor degradation [7]. Such materials can undergo wet processing and are fully compatible with a flexible OLED display fabrication process. In effect, the development of organic materials and fabrication processes may now be at a more mature juncture than that of low temperature amorphous TFT devices for flexible substrate implementation. As a result, organic transistor driver circuits for AMOLED displays become increasingly viable choices for vertically integrated highly flexible display applications.

In this paper, we present the results of evaluating AM display drivers using empirical device models implemented in the circuit simulation software tool SPICE. Device parameters are extracted from measured characteristics of internally fabricated OTFTs and fitted to an appropriate SPICE model, and α-Si SPICE parameters are taken from the recent literature. Our modeling approach is described in more detail in Section II. Circuit simulations are run to estimate the performance of AMOLED drivers based on these transistors. The simulations provide a viable platform to compare and contrast the performance of α-Si and pentacene device in three different driver topologies. Simulations are detailed in Section III. Simulation results presented in Section IV serve to illustrate both the relative performance of Organic and α-Si TFTs and the merits and challenges of the traditional voltage programmed 2-TFT and current programmed 4-TFT circuits. Section V draws inferences about the performance tradeoffs of the 5 TFT circuit.

II. Device Models

SPICE simulates circuit behavior based on mathematical models for discrete electronic devices. Built-in models for common devices at various complexity levels are available to the circuit designer, and the choice of model type for a particular device depends on the level of detail of characterization data available for that device.

The device models provided with the SPICE software are commonly intended for circuit simulations of single crystal Si devices, which are used in most mainstream microelectronics circuits. For this work we adapted the parameters inherent to these SPICE models to α-Si and OTFTs. Device parameters for industrial α-Si transistors are readily available [9], [10]. An empirical fit made to locally measured characteristics from devices fabricated in our laboratory (Georgia Tech) provides the corresponding parameters for pentacene OTFTs. Details of the model parameters are included later in this section.

TABLE I
Device Characteristics

Parameter	α-Si High-Temp Process [11]	Pentacene Low Temp Laboratory Process [8]
Threshold V_t	2V	-1V
Mobility μ	1 cm^2/V-s	0.65 cm^2/V-s
C_{ox}	20nF/cm^2	17nF/cm^2

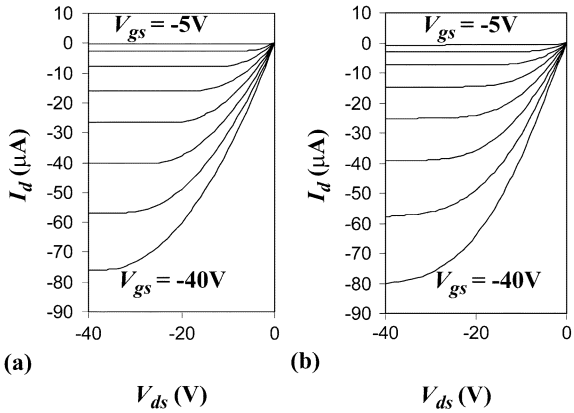

Fig. 1. Pentacene OTFT characteristics shown are (a) modeled and (b) measured characteristics.

The OTFTs modeled in this work have been fabricated on heavily doped n-type Si wafers with a thermally grown SiO_2 layer as gate dielectric (200 nm). Ti (10 nm)/Au (100 nm) source-and-drain contacts were evaporated and the channels defined using lift-off photolithography. Commercially available pentacene was first purified using zone gradient sublimation and then thermally evaporated onto the source/drain contacts at a rate of 0.2 Å/s and at a pressure below 10^{-7} Torr. Details of the device fabrication are described elsewhere [8]. Current–voltage characteristics (drain current I_d versus drain–source voltage $V_{\rm ds}$ at multiple constant gate–source voltages $V_{\rm gs}$) and transfer characteristics (I_d versus $V_{\rm gs}$ at fixed $V_{\rm ds}$) of the transistors are measured in a nitrogen glove box (O_2, H_2 O < 1 ppm) using an Agilent E5272A medium-power source/monitor unit connected to a probe station. The field-effect mobility μ and threshold voltage V_t are then extracted from the transfer characteristic by fitting the square-root of drain current I_d against gate–source voltage $V_{\rm gs}$ using the equation

$$I_d = \mu \frac{CW}{2L}(V_{\rm gs} - V_t)^2 \tag{1}$$

where C is the capacitance per unit area of the gate dielectric (F/cm^2), W the width and L the length of the channel. The values so extracted are shown in Table I.

An example of measured and fitted OTFT current–voltage characteristics is shown in Fig. 1. The figures show reasonable agreement between device data and the fitted device models used in SPICE. The modeling inaccuracies are of the order of

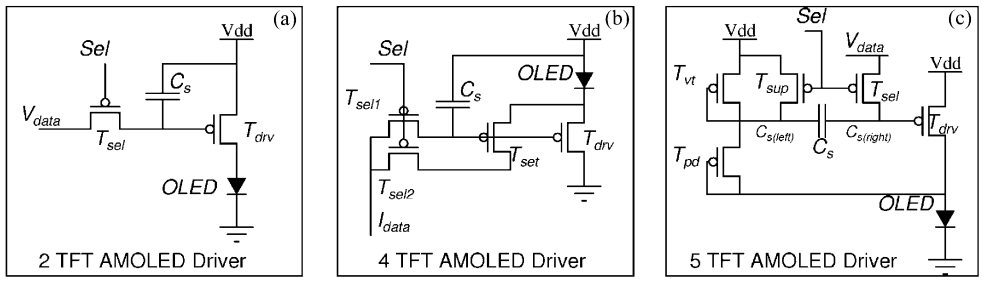

Fig. 2. AMOLED circuits shown are (a) 2-TFT, (b) 4-TFT, and (c) 5-TFT AMOLED driver circuits.

10%–15%. This accuracy can be improved by using more detailed models. However any Si MOS parameters included to explain the characteristics of the OTFT output curves would not correspond to physical processes of the OTFTs since their operation differs from Si FETs. Importantly, in this work the relative performance of circuits is compared, and for this purpose the 15% error in modeled characteristics is tolerable without compromise to our conclusions. A parallel effort to develop more accurate models for OTFTs based on their underlying physics continues in our group for applications requiring more accurate simulations.

Table I summarizes the high temperature α-Si transistor and the fitted pentacene transistor device-level model parameters used to generate the circuit performance figures discussed in this paper. It should be noted that the α-Si device parameters used in these simulations are extracted from an industry optimized high temperature process, while the OTFT devices parameters are taken from models fitted to devices fabricated in a research laboratory. As can be seen in Table I, an incidental similarity occurs between the two types of devices, showing that the gap between OTFT and α-Si TFT process technologies is closing.

III. Circuit Design and Simulation

The main objective of display circuit design is to maximize display performance, including high brightness levels, good uniformity, low power consumption, and low component count with fewer external signals. The three AMOLED driver circuits of this study are presented in Fig. 2, using p-type devices as required for pentacene OTFTs. The same circuits would be configured using n-type TFTs in α-Si technology. Fig. 2(a) shows a well- known two transistor driver configuration, Fig. 2(b) describes a four transistor driver circuit from the literature, while Fig. 2(c) shows a novel five transistor driver configuration. All circuits have devices of length of 20 μm, except for $T_{\rm pd}$ in Fig. 2(c) which needs to be a low conductance (g_m) device and has a length of 40 μm. The driver transistors had a W/L ratio of 25. The $T_{\rm sel}$ transistors in all circuits had W/L of 5. $T_{\rm sel2}$ and $T_{\rm set}$ in Fig. 2(b) were as wide as the driver, with $(W/L = 25)$. $T_{\rm vt}$ and $T_{\rm pd}$ in Fig. 2(c) had W/L ratios of 5 and 1/2, respectively. The sizes chosen for the drive transistor $T_{\rm drv}$ and others that conduct similar values of current including $T_{\rm sel2}$ and $T_{\rm set}$ in Fig. 2(b) were determined from current requirements of each pixel. The select transistors were sized to be able to drive the storage capacitance to required voltage levels within a programming time of 35 μs (Color VGA resolution requirement).

A. Voltage-Driven 2-TFT AMOLED Driver

The 2-TFT driver [Fig. 2(a)] is one of the simplest possible AM driver configurations, and one of the first proposed for both LCD and OLED AM displays. This circuit consists of an OLED driver transistor $T_{\rm drv}$, a select transistor $T_{\rm sel}$, and a storage capacitor C_S, and has been used with both α-Si TFTs [9], [10] and OTFTs [11], [12]. In either case, the 2-TFT circuit works as follows: $T_{\rm drv}$ determines the final current through the OLED based on its gate–source voltage. $T_{\rm sel}$ sets this voltage equal to $V_{\rm data}$ when the pixel select (Sel) line is active. In this way, $V_{\rm data}$ directly determines OLED current (and hence OLED brightness) depending on the $V_{\rm gs} - I_d$ transfer characteristics of $T_{\rm drv}$.

Using a Si transistor approximation and making a reasonable assumption that $T_{\rm drv}$ is in saturation, the OLED current becomes

$$I_D = K(V_{\rm gs} - V_t)^2 \tag{2}$$

with K a constant, $V_{\rm gs}$ the gate–source voltage, and V_t the threshold voltage of the transistor. The current I_D through the OLED is very dependent on the parameters (K, V_t) of the driving transistor, Thereore, the 2-TFT AMOLED is extremely sensitive to operating changes in transistor $T_{\rm drv}$.

Both α-Si [13], [14] and OTFTs, are known to degrade over time [16], and degradation manifests itself most frequently as a threshold voltage increase or mobility reduction. When used in a simple 2-TFT circuit, the threshold voltage variation of the TFTs directly affects brightness levels and pixel uniformity, subsequetly decreasing operational lifetime and increasing power consumption of the AMOLED display.

B. Current-Driven 4-TFT AMOLED Driver

The 4-TFT circuit shown in Fig. 2(b), [4], [9], [17], [10] was conceived as an improvement over the 2-TFT circuit to make OLED brightness relatively independent of the transfer characteristics of $T_{\rm drv}$. The circuit consists of two select transistors $T_{\rm sel1}$ and $T_{\rm sel2}$, a storage capacitor C_s, an OLED drive transistor $T_{\rm drv}$, and a current setting transistor $T_{\rm set}$, with the last two devices being equal in size.

The purpose of this circuit is to directly program the required current in the OLED and let the circuit adjust node voltages to suit this current. Therefore, when Sel goes low, $I_{\rm data}$ is forced through $T_{\rm sel1}$ and $T_{\rm sel2}$. The current through $T_{\rm sel1}$ causes charging of the storage capacitor C_s, while current through $T_{\rm sel2}$ is limited by the initial low conduction of $T_{\rm set}$. As C_s charges, the gate voltage of $T_{\rm set}$ drops until it turns on

sufficiently to conduct all of $I_{\rm data}$. The entire input current is then routed to the OLED. In this way, the gate voltage of $T_{\rm set}$ adjusts itself to allow a current equal to $I_{\rm data}$ to flow through the OLED regardless of the mobility or V_t in the transistor $T_{\rm set}$. Display uniformity across the AMOLED panel is maintained as $I_{\rm data}$ in the OLED remains constant, even when Sel turns off due to the storage capacitor and the mirror action of $T_{\rm drv}$. Thus, the circuit achieves relative independence from changes in V_t, mobility, and most other device parameters that may be degrade over time.

However, the current available to charge the storage capacitor is the same as $I_{\rm data}$. Since $I_{\rm data}$ determines the brightness of the pixel, the charge rate of C_s is proportional to the brightness level. Hence, less bright pixels in a display can be slower to stabilize than the brighter pixels. In addition, the 4-TFT circuit requires $T_{\rm sel2}, T_{\rm set}$ and $T_{\rm drv}$ to be of similar large size in order to carry $I_{\rm data}$, thus reducing the area available to the OLED and limiting the pixel density of a given AMOLED display. Improvements have been proposed to the 4-TFT design with $T_{\rm sel2}, T_{\rm set}$ made smaller than $T_{\rm drv}$, giving an amplifying current mirror $T_{\rm set} - T_{\rm drv}$. These approaches imply that the programming current is also scaled down in the same ratio as $T_{\rm drv}/T_{\rm set}$, leading to further degradation in charging time of C_s and circuit speed.

C. Voltage-Driven 5-TFT AMOLED Driver

Often, the variation in transistor threshold voltage affects device performance more seriously than mobility variation in AMOLED driver circuits [10], [18] although the two parameters are related. In order to validate this observation, we performed an experiment for degradation of an OFET over time. The results are presented in Fig. 3(a). The arrows indicate the direction of change in the characteristics of each curve with degradation. As can be seen from the figure, bias stress causes more of a shift in the $V_{\rm gs} - I_d$ characteristics, rather than change its slope. This translates into a V_t change from -0.68 V to -4.36 V and mobility change from 0.21 cm^2/V-s to 0.22 cm^2/V-s. The values confirm that threshold voltage degradation is more severe as compared to mobility change. The slight increase in mobility is within measurement error.

Since V_t degradation is one of the main symptoms of TFT degradation over time, V_t-independence is a key requirement for uniform emission and small pixel-to-pixel variation of an AMOLED display circuit. To address this critical issue, the proposed 5-TFT AMOLED driver circuit shown in Fig. 2(c) uses a voltage programming compensation approach that attempts to minimize the number of additional TFTs, resulting in a smaller overall circuit area without sacrificing V_t-independence (as with the 2 TFT circuit) or speed (as with the 4 TFT circuit). This circuit consists of five transistors: a drive transistor $T_{\rm drv}$, a select transistor $T_{\rm sel}$, a supply transistor $T_{\rm sup}$, a pull-down transistor $T_{\rm pd}$, and a V_t-compensating transistor $T_{\rm vt}$; as well as a storage capacitor C_s.

When Sel is active (low) at the beginning of the program cycle, $T_{\rm sup}$ charges up $C_{s(\rm left)}$ to *Vdd* while $T_{\rm sel}$ places $V_{\rm data}$ on $C_{s(\rm right)}$. When Sel switches off (high) at the end of the program cycle, the pull down action of weak transistor $T_{\rm pd}$ causes the $C_{s(\rm left)}$ voltage to fall. When a threshold voltage drop is established across the gate–source of $T_{\rm vt}$, it prevents the $C_{s(\rm left)}$ voltage from falling further so that it always falls through voltage V_t at the end of each program cycle. Since voltage on $C_{s(\rm right)}$ is floating when Sel is off, it too falls through the same voltage V_t, and the final voltage on the gate of $T_{\rm drv}$ becomes $V_{\rm data} - V_t$. The bias on $T_{\rm drv}$ is adjusted by a voltage equal to V_t for all input voltages. Since both $T_{\rm drv}$ and $T_{\rm vt}$ are in saturation under normal operation, their threshold voltage degradation should occur at roughly the same rate, thereby providing V_t-independence (of the driver current) for the 5-TFT driver circuit. One consequence of this configuration is that even when $V_{\rm data}$ is '0' or the pixel is OFF, some current flows through $T_{\rm vt}$ and $T_{\rm pd}$ which contributes to current leakage and standby power consumption. The assumption that $T_{\rm drv}$ and $T_{\rm vt}$ degrade at similar rates is central to the V_t compensation scheme of this circuit. In order to test the assumption of comparable degradation in OFETs stressed for the same time, we performed an experiment with pairs of OFETs with the same size, laid out in close proximity and stressed at the same bias and (consequently) current density. The tests were performed on OFET pairs with various W/L ratios, of which the results

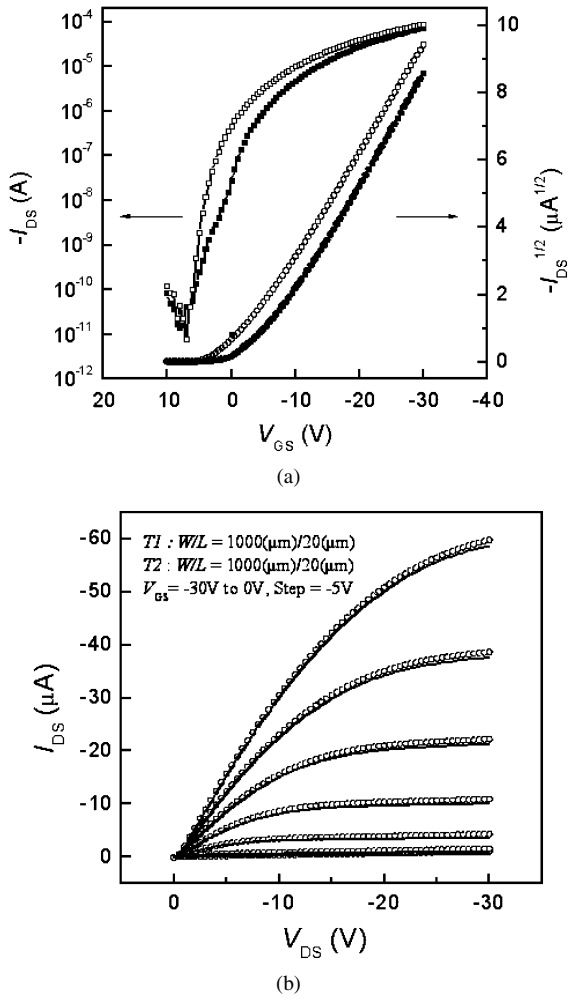

Fig. 3 (a) Single OTFT characteristics before (hollow squares) and after degradation (solid squares). (b) Comparison of output curves of matched TFTs after degradation (still matched).

TABLE II
AREA CONSUMPTION AND DEGRADATION TOLERANCE OF AMOLED DRIVERS

Driver Circuit	Program Method	Circuit Area		Stability (I_{OLED} Change)	
		Total Pixel Area	Fill Factor	100% V_t increase	50% μ decrease[3]
2-TFT	Voltage	7000 μm^2	92%	23.2%	49.6%
4-TFT	Current	22500[1] μm^2	75%	0.4%[2]	0.0%
5-TFT	Voltage	14400 μm^2	84%	5.9%	47.3%

1. Area of classical 4-TFT circuit. Recent work has used asymmetrical current mirrors to reduce size of all but the driving TFT, leading to area only slightly larger than the 2-TFT
2. Assumes perfect column current, which is a challenge with low current values encountered at high grey scale depths
3. The 5-TFT circuit is designed to compensate for threshold voltage variation, *not* mobility variation. The former is dominant in many cases [22]

TABLE III
SPEED COMPARISON OF AMOLED DRIVERS

Driver Circuit	Transistor Technology	Speed	
		Program Time	Switch-off Time
2-TFT	α-Si	40μs	6μs
	Pentacene	60μs	10μs
4-TFT	α-Si	100μs	6μs
	Pentacene	120μs	10μs
5-TFT	α-Si	50μs	6μs
	Pentacene	70μs	10μs

for the $W/L = 1000/20$ pair are shown in Fig. 3(b). The degradation in both transistors of each mirror circuit with bias stress was thus found to be closely comparable, consistently over the entire set of test transistors, which led to almost identical characteristics for both transistors before and after degradation.

IV. SIMULATION RESULTS

In order to quantitatively estimate the characteristics of the three active driver circuits described in Section III, we perform a series of SPICE simulations using the α-Si and OTFT device models described in Section II of this article. These simulations yield first order estimates for speed, power, circuit area and V_t degradation independence, or stability. Speed and leakage power results are summarized in Table III, while circuit area and stability are summarized in Table II. The circuits are sized to provide similar drive currents, of about 10 μA with pentacene transistors. Hence, the drive power for full brightness is equal for all circuits. The α-Si circuits are then sized the same as their pentacene counterparts and as as result, generate higher current ($\sim$17 μA) leading to a higher power dissipation.

Speed of these circuits is measured via two transitions. The first is the program time for the establishment of full drive current in the OLED from dark conditions, which involves depositing a certain charge on the storage capacitor. The second time value measured for each circuit is the switch-off time for the opposite transition. Switch off is achieved by connecting the input data line to *Vdd* while the pixel is in program mode, which discharges the storage capacitor completely. Although programming the 4-TFT circuit is current-mode, discharge is voltage mode. Thus, the discharge times for all three circuits are the same, given that the size of the storage capacitor and of the driver transistors is the same.

A feature evident in Table III is the consistently higher speed of α-Si circuits which is a direct result of the higher mobility of these devices. However, it should be noted that the α-Si device parameters used in these simulations are extracted from an industry optimized high temperature process, while the OTFT devices parameters are taken from devices fabricated in a research laboratory. Thus, it is reasonable to expect more favorable performance from an optimized OTFT fabrication process. As discussed in Section I of this article, OTFTs and OLEDs use extremely compatible fabrication processes, often using the same process tools, and OTFTs offer many of the same advantages as OLEDs. In general, the simulation results contained in this article show that OTFT AMOLED display circuit performance is comparable to that of high-temperature α-Si TFT circuits, which makes optimization of OTFT manufacturing processes increasingly attractive for highly flexible display applications.

We can also glean useful information for circuit optimization from Table III. As the simulation shows, the 4-TFT driver circuit is approximately 2 times slower using OTFT devices and 2.5 slower using α-Si TFT devices than the 2- TFT circuit configuration, while the 5-TFT driver circuit is comparable in terms of pixel-on and pixel-off speed to the simple 2-TFT configuration. This result establishes that the 5-TFT circuit retains the speed advantage of the 2-TFT circuit.

Since the program current for the 4-TFT circuit is directly proportional (if not equal) to the drive current of the OLED, the program time for the 4-TFT circuit worsens for low grayscale values of the pixel. The program current for the 2-, 5-TFT circuits is independent of the pixel grayscale value, hence programming is usually faster. A comparison of the program cycle for the three circuits is given in Fig. 4 for similar grayscale values. Each curve represents the current in the OLED in one of the 2-, 4-, and 5-TFT circuits. In addition to speed and power consumption, the active area of each OLED pixel compared to the area taken by each pixel's active driver circuit is an important figure of merit for display applications. Described in the literature as fill factor or pixel aspect ratio and defined as OLED area/total area, it is often more a function of circuit design than of the process technology used to manufacture the

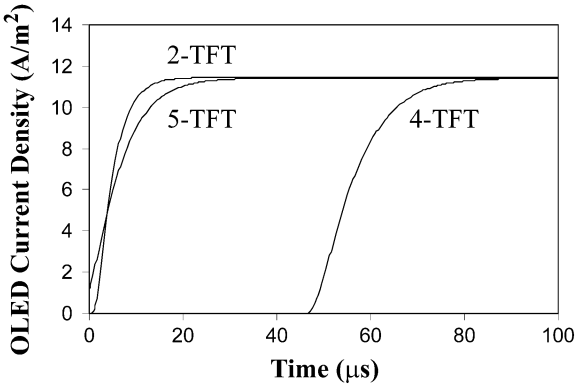

Fig. 4. Transient prformance. Shown are the response times for 2-TFT, 4-TFT, and 5-TFT AMOLED driver circuits. 0 μs corresponds to the start of the program cycle when Sel goes low.

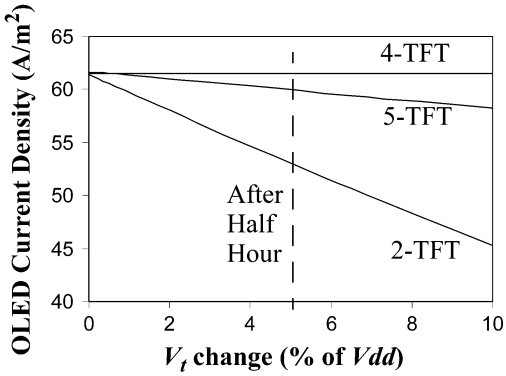

Fig. 5. Circuit response to V_t degradation. Shown is the reduction in OLED current density as a function of degradation in the OFET (as expressed by changes in the threshold voltage as a percentage of V_{dd}).

transistors. As stated in the description of Table II, to derive the results shown, the area required to sustain approximately 10 μA through the OLED pixel has been determined empirically, using an industry standard OLED size of 300 μm $\times$ 300 μm to compute the fill factor. As expected, the highest fill factor is seen with the simplest device driver configuration, the 2-TFT circuit. The smallest fill factor is seen for the 4-TFT circuit configuration. In the 4-TFT circuit, it is possible to reduce the area of transistors (and hence increase fill factor) by introducing asymmetry in the $T_{\rm set}$ and $T_{\rm drv}$ mirror pair, sizing all components much smaller than $T_{\rm drv}$, and by using current amplification between $T_{\rm set}$ and $T_{\rm drv}$, resulting in an increase of fill factor comparable to that of the 5-TFT circuit [20]. However, the slighly smaller fill factor of the 5-TFT circuit is well compensated by a significant improvement in programming speed compared to the 4-TFT circuit.

The final metric in Table II is a measure of degradation tolerance of the three circuit topologies. Two types of degradation are individually forced on the device models: 1) a V_t increase of 100% (from the original model-fit value of 1 V to a degraded value of 2 V); and 2) a mobility decrease of 50% (from the model fit value of 0.65 cm^2/V-s to 0.325 cm^2/V-s). The change in drive current with change in V_t is tabulated as a percentage of the original value. The change of OLED current density with degradation in V_t is also plotted in for illustration of V_t-degradation tolerance of the the AMOLED drivers. A change in V_t of 2 V corresponds to a change with respect to V_{dd} (20 V) of 10%, which is the extent of the X axis of Fig. 5.

When bias stress degradation measurements were conducted on our devices as shown in Fig. 3, we found a rate of degradation that would put the half hour degradation point at the vertical dashed line in Fig. 5.

Because device degradation can affect performance of OTFTs and because such effects may be reduced by intelligent circuit design, a metric for stability is defined and calculated for each of the three circuit configurations. For purposes of this discussion, stability is defined in terms of fractional drive current change for a 1-V change in threshold voltage for all OFETs in a given circuit. As expected from the circuit description in Section III of this article, Table II indicates that the 2-TFT circuit performs the worst in terms of V_t stability. The 4-TFT circuit is relatively insensitive to the V_t change due to its current programming scheme, while the 5-TFT circuit improves considerably on the 2-TFT circuit for V_t degradation tolerance. Fig. 5 shows a trend for change in output drive current with change in V_t up to 100%. The 2-TFT circuit has the maximum change in current while the 4-TFT is almost immune to degradation.

This immunity however, is of a limited nature. As the threshold voltage degrades, the storage capacitor will require a longer charging cycle to reach a voltage sufficient to drive the same current. Thus, the response time of the circuit will deteriorate. Also, the immunity presented above is contingent on the assumption that both the $T_{\rm set}$ and $T_{\rm drv}$ transistors degrade at the same rate. If the degradation for $T_{\rm set}$ is, for example, larger than that for $T_{\rm drv}$, the current driven when programming is switched off will increase with degradation. The 5-TFT circuit again shows a characteristic close to the 4-TFT circuit. Degradation due to threshold voltage change dominates over degradation due to mobility change [22]. The 5-TFT circuit is thus designed specifically to compensate for threshold voltage change. In processes where mobility change is significant, the 5-TFT performance is equivalent to the 2-TFT circuit. Of the circuits evaluated here, the 2-TFT circuit is the simplest and thus has the highest speed and fill factor, but does not correct for degradation of threshold voltage. The 4-TFT circuit adds device parameter and degradation independence at the cost of speed due to the limited data current available to charge C_s. Although the best scheme in terms of immunity to degradation, the 4-TFT circuit potentially decreases fill factor and can cause low brightness areas of a display to be slow, limiting overall speed and frame rate. Finally, the 5-TFT circuit achieves a better speed-stability compromise especially at low output brightness levels. It's voltage programming speed makes it as fast as the 2-TFT circuit, and the circuit topology adds the desired property of V_t-independence and increased fill factor, while adding a small amount of complexity and an increase in standby power consumption of only 1% of full-brightness power. Thus, if a display consumes 100 mW with all pixels fully 'white', the 5 TFT display would dissipate 1 mW as quiescent power with the 5-TFT scheme. If 50% pixels were white on an average, the display would still only dissipate 2% of the total display power. This quiescent power consumption can be further reduced by carefully sizing the V_t-compensating transistors.

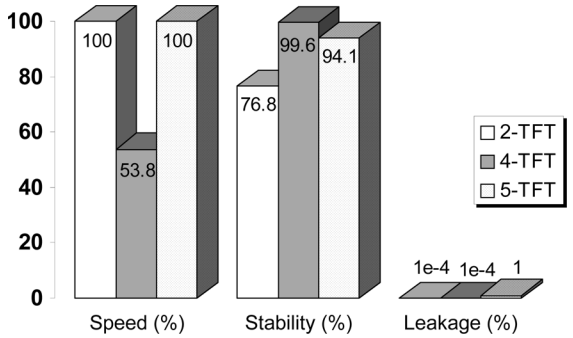

Fig. 6. Performance summary. Comparison of AMOLED driver circuits with regards to relative program speed, Immunity to V_t degrdation of 100% and standby power consumption as a fraction of full-brightness power.

V. Results and Discussion

Results predict that OTFTs are promising candidates for driving AMOLED displays to required luminance levels. The performance of these transistors even in laboratory research fabrication conditions comes within 66% of their high-temperature α-Si, counterparts, which is currently the industry standard for active display transistors. The performance lag occurs almost exclusively from lower mobility measured in the locally fabricated devices, which is a parameter that is evolving with newer generation OTFTs. Further, as noted in [11] the aspect ratio or fill factor of an AMOLED pixel with current OLED efficiencies is not a significant function of mobility above $\sim$0.1 cm^2/V-s range, which OTFTs have already achieved. Thus, OTFTs make a strong case for investigation as AMOLED drivers with future promise of integration with highly flexible substrates.

Moreover, newer circuit topologies can mitigate the OTFT disadvantages of low mobility and high degradation, while allowing industry to take advantage of combined OTFT/OLED process integration, especially for highly flexible display applications. One such circuit configuration is the 5-TFT circuit presented here. Simulation results indicate that the 5-TFT circuit combines the speed of voltage programming even at low output brightness levels with the desired property of V_t-independence, while adding negligible complexity and an increase in standby power consumption up to 1% of the 'ON' power of each pixel. This performance tradeoff is summarized in Fig. 6.

In summary, the 5-TFT circuit enables the use of fast voltage programming and potentially better grayscaling for AMOLED displays even in the face of V_t-degradation of the OTFTs, which was not possible in earlier topologies.

References

[1] H. Gleskova, S. Wagner, V. Gasparik, and P. Kovac, "150 °C amorphous silicon thin-film transistor technology for polyimide substrates," *J. Electrochem. Soc.*, vol. 148, no. 7, pp. 370–374, Jul. 2001.

[2] A. Sazonov, D. Striakhilev, C.-H. Lee, and A. Nathan, "Low-temperature materials and thin-film transistors for flexible electronics," *Proc. IEEE*, vol. 93, no. 8, pp. 1420–1428, Aug. 2005.

[3] T. W. Kelley, P. F. Baude, C. Gerlach, D. E. Ender, D. Muyres, M. A. Haase, D. E. Vogel, and S. D. Theiss, "Recent progress in organic electronics: Materials, devices, and processes," *Chem. Mater.*, vol. 16, no. 23, pp. 4413–4422, Nov. 16, 2004.

[4] G. H. Kim, J. Oh, Y. S. Yang, L.-M. Do, and K. S. Suh, "Encapsulation of organic light-emitting devices by means of photopolymerized polyacrylate films," *Polymer*, vol. 45, no. 6, pp. 1879–1883, Mar. 15, 2004.

[5] A. Kumar, A. Nathan, G. E. Jabbour, H. K. Baik, W. J. Kim, W. H. Koo, S. J. Jo, C. S. Kim, J. Lee, and S. Im, "Enhancement of long-term stability of pentacene thin-film transistors encapsulated with transparent SnO_2," *Appl. Surf. Sci.*, vol. 252, no. 5, pp. 1332–1338, Dec. 15, 2005.

[6] S. H. Han, J. H. Kim, J. Jang, S. M. Cho, M. H. Oh, S. H. Lee, and D. J. Choo, "Lifetime of organic thin- film transistors with organic passivation layers," *Appl. Phys. Lett.*, vol. 88, no. 7, pp. 73519-1–73519-3, Feb. 13, 2006.

[7] J. S. Lewis and M. S. Weaver, "Thin-film permeation-barrier technology for flexible organic light-emitting devices," *IEEE J. Sel. Top. Quant. Electron.*, vol. 10, no. 1, pp. 45–57, Jan.–Feb. 2004.

[8] J. N. Haddock, X. Zhang, S. Zheng, Q. Zhang, S. R. Marder, and B. Kippelen, "A comprehensive study of short channel effects in organic field-effect transistors," *Org. Electron.*, vol. 7, pp. 45–54, 2006.

[9] S. Wagner, H. Gleskova, I.-C. Cheng, and M. Wu, "Silicon for thin-film transistors," *Thin Solid Films*, vol. 430, no. 1–2, pp. 15–19, Apr. 22, 2003.

[10] S. Sambandan, K. Sakariya, P. Servati, A. Kumar, and A. Nathan, "Voltage programmed pixel driver circuits for AMOLED applications: Design optimization of pixel select and drive stages," *Proc. SPIE*, vol. 5363, no. 1, pp. 16–26, Jun. 25, 2004.

[11] A. Kumar, A. Nathan, and G. Jabbour, "Does TFT mobility impact pixel size in AMOLED backplanes?," *IEEE Trans. Electron. Devices*, vol. 52, no. 11, pp. 2386–2394, Nov. 2005.

[12] L. Zhou, A. Wanga, S.-C. Wu, J. Sun, S. Park, and T. N. Jackson, "All-organic active-matrix flexible display," *Appl. Phys. Lett.*, vol. 88, no. 8, p. 083502, 2006.

[13] L. Zhou, S. Park, B. Bai, J. Sun, S.-C. Wu, T. N. Jackson, S. Nelson, (K.) D. Freeman, and Y. Hong, "Pentacene TFT driven AM OLED displays," *IEEE Electron Device Lett.*, vol. 26, no. 9, pp. 640–642, Sep. 2005.

[14] M. J. Powell, C. van Berkel, and J. R. Hughes, "Time and temperature dependence of instability mechanisms in amorphous silicon thin-film transistors," *Appl. Phys. Lett.*, vol. 54, no. 14, pp. 1323–1325, Apr. 3, 1989.

[15] A. R. Merticaru, A. J. Mouthaan, and F. G. Kuper, "Progressive degradation in a-Si:H/SiN thin-film transistors," *Thin Solid Films*, vol. 427, no. 1–2, pp. 60–66, Mar. 3, 2003, (Twente Univ., Enschede, Netherlands);.

[16] Y. Qiu, Y. Hu, G. Dong, L. Wang, J. Xie, and Y. Ma, "H_2O effect on the stability of organic thin-film field- effect transistors," *Appl. Phys. Lett.*, vol. 83, no. 8, pp. 1644–1646, Aug. 25, 2003.

[17] Y. H. Kim, S. K. Park, J. I. Han, D. G. Moon, and W. K. Kim, "Investigation of stability in polymer thin-film transistors for flexible active-matrix displays," *Proc. SPIE*, vol. 5464, pp. 298–305, 2004.

[18] S. Ono and Y. Kobayashi, "Four-thin-film-transistor pixel circuit for amorphous-silicon active-matrix organic light-emitting diode displays," *Jap. J. Appl. Phys.*, vol. 43, no. 12, pt. 1, pp. 7947–7952, Dec. 2004.

[19] A. Nathan, G. R. Chaji, and S. J. Ashtiani, "Driving schemes for a-Si and LTPS AMOLED displays," *J. Display Technol.*, vol. 1, no. 2, pp. 267–277, Dec. 2005.

[20] K. Sakariya, S. Sambandan, P. Servati, and A. Nathan, "Analysis and characterization of self-compensating current programmed a-Si:H active-matrix organic light-emitting diode pixel circuits," *J. Vacuum Science Technol. A* , vol. 22, no. 3, pp. 1001–1004, May 2004.

[21] H. S. Pae, Y. S. Na, O. K. Kwon, and H. S. Kim, "Driving Circuit of Active-Matrix Method in Display Device," U.S. Patent #6 917 350 B2, Jul. 12, 2005.

[22] R. M. A. Dawson, Z. Shen, D. A. Furst, S. Connor , J. Hsu, M. G. Kane, R. G. Stewart, A. Ipri, C. N. King, P. J. Green, R. T. Flegal, S. Pearson, W. A. Barrow, E. Dickey, K. Ping, S. Robinson, C. W. Tang, S. Van Slyke, F. Chen, J. Shi, M. H. Lu, and J. C. Sturm, "The impact of the transient response of organic light emitting diodes on the design of active-matrix OLED displays," in *Int. Electron Devices Meeting Tech. Dig.,* , 1998, pp. 875–878.

Vaibhav Vaidya (S'04) received the Bachelor's degree from Goa Engineering College, Ponda, India, in 2003. He is working toward the Ph.D. degree at the Distributed Microsystems Laboratory, University of Washington, Seattle.

His current research focuses on organic thin-film devices and circuits, with a stress on developing circuits for active-matrix displays and extending the application base of organic circuits with innovative integration approaches.

Susan Soggs received B.S. degree in chemical engineering and the M.S. degree in electrical engineering the from the University of Washington, Seattle, in 1994 and 2004, respectively.

She has extensive work experience with Motorola Semiconductor Products Sector and U.S. Navy microwave communications. Her research interests are in process integration and device modeling, particularly as they relate to organic materials and devices.

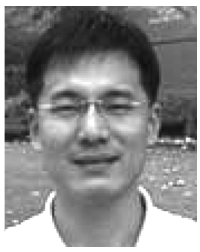

Jungbae Kim received the B.S. and M.S. degrees in electrical engineering from Kyungpook National University, Daegu, Korea, and Seoul National University, Seoul, Korea, in 1993 and 1997, respectively. He is currently working on the Ph.D. degree in electrical and computer engineering at the Georgia Institute of Technology in Atlanta, GA.

He is working on organic thin-film transistors and active-matrix organic light-emitting diode (OLED) display. He was a Research Engineer in OLED group at LG Institute of Technology from 1997 to 2002.

Andreas Haldi received the diploma in interdisciplinary science from the Federal Institute of Technology ETH Zurich, Switzerland, in 2003. He is currently working towrd the Ph.D. degree in electrical engineering at the Georgia Institute of Technology in Atlanta, GA,

He is working on organic light-emitting diodes with a main focus on electrophosphorescent devices.

Joshua N. Haddock received the B.S. degree in optical engineering from the University of Rochester, Rochester, NY,in 1998 and the M.S. and Ph.D. degrees in optical sciences from the College of Optical Sciences, University of Arizona, Tucson, in 2000 and 2005, respectively.

His research interests include liquid crystalline materials and devices, organic light-emitting diodes, organic field-effect transistors, and hybrid organic/inorganic high-k dielectric materials for organic electronics applications.

Bernard Kippelen was born and raised in Alsace, France. He received the Maitrise in solid-state physics from the University Louis Pasteur, Strasbourg, France, and the Ph.D. degree in nonlinear optics in 1985 and 1990, respectively.

From 1990 to 1997, he was Chargé de Recherches at the CNRS, France. In 1994, he joined the faculty of the Optical Sciences Center, University of Arizona, Tucson. Since August 2003, he has been a Professor in the School of Electrical and Computer Engineering, Georgia Institute of Technology, Atlanta, where his research ranges from the investigation of fundamental physical processes (nonlinear optical activity, charge transport, light harvesting and emission) in organic nanostructured thin films, to the design, fabrication and testing of light-weight flexible optoelectronic devices based on organic-based materials. He serves as Associate Director of the Center for Organic Photonics and Electronics and as Associate Director of the National Science Foundation Science and Technology Center MDITR.

Denise M. Wilson (M'89) was born in Chicago, IL, in 1966. She received the B.S. degree in mechanical engineering from Stanford University, Stanford, CA, in 1988, and the M.S. and Ph.D. degrees in electrical engineering from the Georgia Institute of Technology, Atlanta, in 1989 and 1995, respectively.

She is currently an Associate Professor with the Electrical Engineering Department, University of Washington, Seattle, and she was previously with the University of Kentucky, Lexington, in a similar position from 1996 to 1999. She was also with Applied Materials, a semiconductor capital equipment supplier, from 1990 to 1992. Her research interests focus on the development of signal processing architectures, array platforms, and other infrastructures for visual, auditory, and chemical-sensing microsystems.